Microsymbiont discrimination mediated by a host-secreted peptide in *Medicago truncatula*

Shengming Yang[a,1], Qi Wang[a,1], Elena Fedorova[b], Jinge Liu[a], Qiulin Qin[a], Qiaolin Zheng[a], Paul A. Price[c,d], Huairong Pan[e], Dong Wang[e], Joel S. Griffitts[c], Ton Bisseling[b], and Hongyan Zhu[a,2]

[a]Department of Plant and Soil Sciences, University of Kentucky, Lexington, KY 40546; [b]Laboratory of Molecular Biology, Graduate School of Experimental Plant Sciences, Wageningen University, 6708 PB Wageningen, The Netherlands; [c]Department of Microbiology and Molecular Biology, Brigham Young University, Provo, UT 84602; [d]Department of Biology, Eastern Michigan University, Ypsilanti, MI 47197; and [e]Department of Biochemistry and Molecular Biology, University of Massachusetts, Amherst, MA 01003

Edited by Graham C. Walker, Massachusetts Institute of Technology, Cambridge, MA, and approved May 23, 2017 (received for review January 11, 2017)

The legume–rhizobial symbiosis results in the formation of root nodules that provide an ecological niche for nitrogen-fixing bacteria. However, plant–bacteria genotypic interactions can lead to wide variation in nitrogen fixation efficiency, and it is not uncommon that a bacterial strain forms functional (Fix^+) nodules on one plant genotype but nonfunctional (Fix^-) nodules on another. Host genetic control of this specificity is unknown. We herein report the cloning of the *Medicago truncatula NFS1* gene that regulates the fixation-level incompatibility with the microsymbiont *Sinorhizobium meliloti* Rm41. We show that *NFS1* encodes a nodule-specific cysteine-rich (NCR) peptide. In contrast to the known role of NCR peptides as effectors of endosymbionts' differentiation to nitrogen-fixing bacteroids, we demonstrate that specific NCRs control discrimination against incompatible microsymbionts. *NFS1* provokes bacterial cell death and early nodule senescence in an allele-specific and rhizobial strain-specific manner, and its function is dependent on host genetic background.

legumes | nodulation | nitrogen fixation specificity | symbiosis persistence | NCR peptides

Plants of the legume family can supply their own nitrogen needs through symbioses with nitrogen-fixing soil bacteria called rhizobia. This symbiotic interaction commences when the host perceives rhizobial lipo-chitooligosaccharides known as nodulation (Nod) factors and initiates development of nodule primordia that become infected by the rhizobia (1). Infection of most legumes, including the model legume *Medicago truncatula*, starts in root hairs and involves formation of plant-made tubular structures known as infection threads (2). Infection threads direct bacteria to these primordia, where the rhizobia are released into the cytoplasm of host cells. During this process, the bacteria become surrounded by a host membrane, and these membrane compartments containing rhizobium are named symbiosomes. Subsequently, the rhizobia differentiate into nitrogen-fixing bacteroids (3).

The legume–rhizobial symbiosis shows a high level of specificity, occurring at both species and genotypic levels (4, 5). Incompatible interactions at initial stages of the association can block bacterial infection and nodule organogenesis. This incompatibility can be caused by failed Nod factor or exopolysaccharide recognition (6–9) or by induced plant immune responses (9–11). Symbiotic incompatibility also takes place at later stages of nodule development, resulting in the formation of infected but nonfunctional nodules (12, 13). This latter situation is well-documented in the *Medicago–Sinorhizobium* symbiosis, in which the bacteria undergo terminal differentiation (14). We previously screened a core collection of *Medicago* accessions using multiple *Sinorhizobium meliloti* strains, evaluating many host–strain combinations (13). In that experiment, ∼40% of the plant–strain combinations produced small, white infected nodules that were defective in nitrogen fixation (Fix^-) whereas only ∼2% resulted in a nonnodulating phenotype (Nod^-). This outcome indicates that natural variation in symbiotic specificity is most pronounced at the nitrogen-fixing phase of nodule development; yet very little is known about the molecular mechanisms of host–strain compatibility during this phase of the symbiosis.

Here, we report the identification and cloning of the *M. truncatula NFS1* gene that controls fixation-level incompatibility with *S. meliloti* Rm41. We used forward and reverse genetic approaches to demonstrate that *NFS1* encodes a nodule-specific cysteine-rich (NCR) peptide that negatively affects symbiotic performance. *NFS1* functions in a context-dependent manner, and its negative role on symbiosis is strain-specific. Our work may lead to development of novel strategies for genetic improvement of symbiotic nitrogen fixation in legumes.

Results and Discussion

We undertook a genetic analysis of the symbiotic specificity involving *S. meliloti* Rm41 using a recombinant inbred line (RIL) population derived from the cross of parental genotypes Jemalong A17 (A17) and DZA315.16 (DZA315) (15). DZA315 forms Fix^+ nodules with Rm41 whereas A17 forms Fix^- nodules with this strain (Fig. 1 *A*–*C*) even though it forms Fix^+ nodules with many other strains such as *Sinorhizobium medicae* strain ABS7 (13). Rm41 bacteria are able to successfully infect and differentiate in A17 nodule cells, but bacteroid lysis and nodule senescence develop very rapidly. Six weeks postinoculation, the Fix^+ nodules of DZA315 contained up to 50 to 55 cell layers, and

Significance

The legume–rhizobial symbiosis culminates in the formation of nitrogen-fixing root nodules. This symbiotic relationship plays a critical role in sustainable agriculture because it reduces the need for nitrogen fertilizers. However, nitrogen fixation efficiency varies tremendously between different plant–bacteria combinations, and the molecular mechanisms that regulate this specificity are not well understood. We report that this specificity is regulated by nodule-specific cysteine-rich (NCR) peptides in *Medicago truncatula*, a model legume closely related to alfalfa (*Medicago sativa*). Our finding provides insights into cross-kingdom signaling in host–bacterial symbioses and makes NCRs attractive agents for engineering legume–rhizobia pairs to optimize nitrogen fixation performance.

Author contributions: S.Y., Q.W., E.F., and H.Z. designed research; S.Y., Q.W., E.F., J.L., Q.Q., Q.Z., P.A.P., and H.P. performed research; D.W., J.S.G., and T.B. contributed new reagents/analytic tools; S.Y., Q.W., E.F., J.L., Q.Z., P.A.P., H.P., D.W., T.B., and H.Z. analyzed data; and J.S.G. and H.Z. wrote the paper.

The authors declare no conflict of interest.

This article is a PNAS Direct Submission.

[1]S.Y. and Q.W. contributed equally to this work.

[2]To whom correspondence should be addressed. Email: hzhu4@uky.edu.

This article contains supporting information online at www.pnas.org/lookup/suppl/doi:10.1073/pnas.1700460114/-/DCSupplemental.

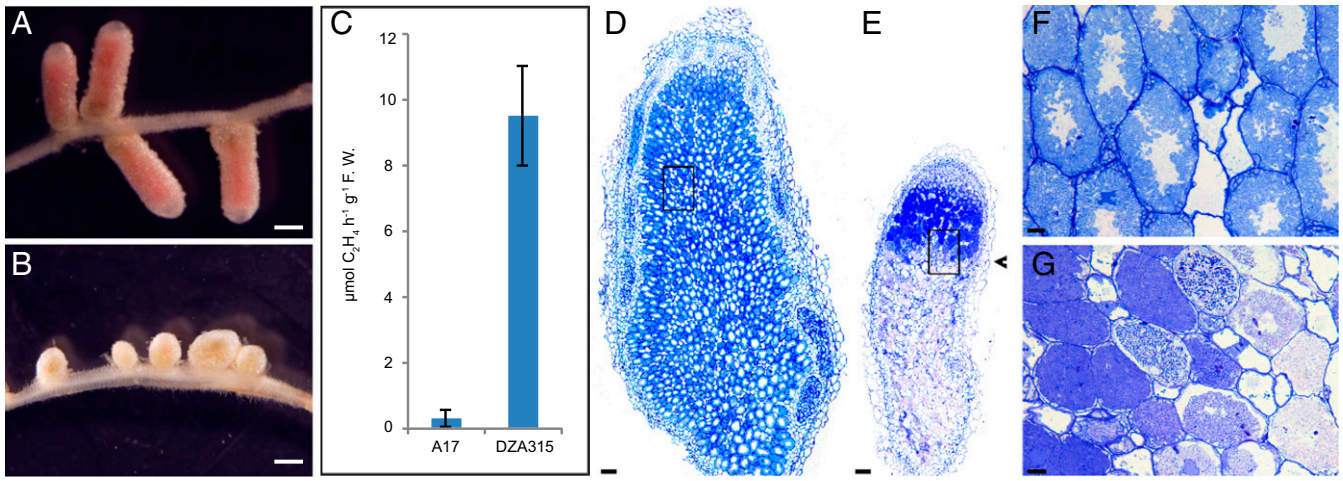

Fig. 1. Nitrogen fixation specificity in *M. truncatula* involving *S. meliloti* Rm41. (*A* and *B*) DZA315 formed elongated pink nodules able to fix nitrogen (Fix^+) (*A*) whereas A17 developed small and white nodules defective in nitrogen fixation (Fix^-) (*B*). (*C*) Acetylene reduction assays ($n = 10$) for the DZA315 (Fix^+) and A17 (Fix^-) nodules, showing a significant difference in *nitrogenase* activity (expressed as μmol C_2H_4 $h^{-1}{\cdot}g^{-1}$ fresh weight, $P < 0.0001$). Bars show the SEM. (*D*–*G*) Light microscopy of a toluidine blue-stained longitudinal section of a Fix^+ nodule of DZA315 (*D* and *F*) and a Fix^- nodule of A17 (*E* and *G*) 6 wk postinoculation. The Fix^+ nodules generally comprised 50 to 55 cell layers without senescent cells (*D*). Infected cells contained well-developed symbiosomes radially aligned around the vacuoles (*F*). In the Fix^- nodules of A17, senescence started in 2 to 3 cell layers of the nitrogen-fixing zone (arrowhead) (*E*). Infected cells contained elongated bacteroids, but the vacuoles were not well-developed (*G*). (*F* and *G*) Magnification of the boxed areas in *D* and *E*, respectively. (Scale bars: *A* and *B*, 1 mm; *D* and *E*, 100 μm; *F* and *G*, 12.5 μm.) F.W., fresh weight.

senescence was starting in the most proximal cell layers of the nitrogen-fixing zone (Fig. 1 *D* and *F* and Fig. S1 *A*–*C*). In contrast, in the Fix^- nodules of A17, senescent cells were clearly visible in the first 2 to 3 cell layers of the fixation zone (Fig. 1 *E* and *G* and Fig. S1 *D*–*F*). From a total of 146 RILs inoculated with Rm41, 92 formed Fix^+ nodules and 52 formed Fix^- nodules; two residual heterozygous lines (here called RHL-NFS1 and RHL-NFS2) segregated for both phenotypes (Table S1). The segregation of the Fix^+ and Fix^- phenotypes in the RIL population does not fit the 1:1 ratio expected from a single gene model ($\chi^2 = 11.1$, df = 1, $P = 0.0009$). As described below, we have evidence that the phenotypic difference between the two parents is controlled by multiple genetic loci.

The involvement of multiple genes controlling the nitrogen fixation phenotype posed a challenge for fine mapping of the underlying loci using an F2 or RIL population. Nonetheless, a whole genome scan of the RIL population using molecular markers identified a small region on chromosome 8 that was strongly associated, but not absolutely cosegregating, with the phenotypes (Table S1). We named this locus "nitrogen fixation specificity 1" (*NFS1*). At the *NFS1* locus, all of the 52 Fix^- RILs were associated with the homozygous A17 haplotype whereas 79 of the 92 Fix^+ RILs were affiliated with the homozygous DZA315 haplotype (Phi coefficient $\varphi = 0.83$, $P < 0.0001$). We designated the A17 allele of *NFS1* as $NFS1^-$ and the DZA315 allele as $NFS1^+$.

Fine mapping of the *NFS1* locus was facilitated by the availability of the aforementioned residual heterozygous line, RHL-NFS1, because the segregation of the Fix^+ and Fix^- phenotypes in the progeny of this line resulted from the residual heterozygosity around this locus. Because most other regions of the genome have become homozygous, the progeny of heterozygous

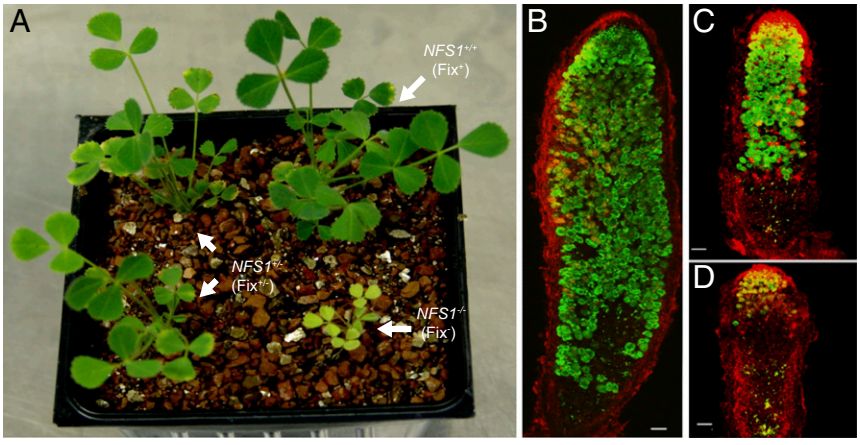

Fig. 2. Segregation of Fix^+, Fix^-, and $Fix^{+/-}$ phenotypes in the progeny of RHL-NFS1. (*A*) Plants forming Fix^+, Fix^-, and $Fix^{+/-}$ nodules were visually distinguishable by their growth vigor. (*B*–*D*) Confocal microscopy of Fix^+ (*B*), $Fix^{+/-}$ (*C*), and Fix^- (*D*) nodules infected by GFP-tagged Rm41. Samples were contrasted with propidium iodide (red). The Fix^+ and Fix^- nodules were structurally similar to those formed on the DZA315 and A17 roots, respectively. The $Fix^{+/-}$ nodules, however, were smaller in size, contained smaller numbers of symbiotic cells, and had an extended zone of senescence compared with the Fix^+ nodules. (*B* and *C*) Prepared with multiple images. (Scale bars: *B*–*D*, 100 μm.)

RHL-NFS1 plants share a nearly identical genetic background (near-isogenic). As expected, the progeny homozygous for the $NFS1^{+}$ allele ($NFS1^{+/+}$) showed the Fix^{+} phenotype, and the plants homozygous for the $NSF1^{-}$ allele ($NFS1^{-/-}$) were Fix^{-}. However, the heterozygotes ($NFS1^{+/-}$) displayed an intermediate phenotype (denoted as $Fix^{+/-}$) (Fig. 2*A*). The $Fix^{+/-}$ nodules were able to fix nitrogen but at much lower efficiency compared with that of the $NFS1^{+/+}$ genotype. The three phenotypes can be unambiguously distinguished from each other based on the size and vigor of the plants (Fig. 2*A*), as well as the nodule size and morphology (Fig. 2 *B*–*D*). The effect of the *NFS1* locus on symbiotic performance is strain-specific; for example, the isogenic $NFS1^{+/+}$ and $NFS1^{-/-}$ plants both formed Fix^{+} nodules when inoculated with *S. medicae* ABS7 (Fig. S2).

Fine mapping using more than 10,000 plants delimited the *NFS1* locus within a 4.9-kb genomic region (Fig. 3*A* and Fig. S3). Annotation of the genomic sequence of DZA315 identified two genes, each of which encodes a nodule-specific cysteine-rich (NCR) peptide (16–18). One of the *NCRs* (*NCR-α*) corresponds to *Medtr8g073380* in A17 whereas the second one (*NCR-β*) was not annotated in the A17 genome because it carries a G-to-A mutation at the intron–exon splicing site compared with the DZA315 allele. *NCRs* represent a large gene family in *M. truncatula* that are expressed in a highly nodule-specific manner (16). Delivery of NCR peptides to symbiosomes has been shown to be essential for the rhizobia to differentiate into nitrogen-fixing bacteroids (17, 18). Therefore, we postulated that *NCR-α* and *NCR-β* were the candidate genes of *NFS1*.

However, the intermediate phenotype displayed by the heterozygotes raised a question of whether only one or both $NFS1^{+}$ and $NFS1^{-}$ alleles contribute to the nitrogen-fixing phenotype. One scenario is that one allele is dominant over another, and the function of the dominant allele (either $NFS1^{+}$ or $NFS1^{-}$) is dosage-dependent (partially dominant). Alternatively, $NFS1^{+}$ and $NFS1^{-}$ contribute to the Fix^{+} and Fix^{-} phenotypes, respectively, and the heterozygotes display blending effects of both alleles (codominant). We therefore tested the function of both alleles of each candidate gene in the near-isogenic background of RHL-NFS1 through hairy root transformation. In light of our current knowledge of the positive role that *NCRs* play in mediating terminal bacterial differentiation and nitrogen fixation (17–23), we first introduced the DZA315 (Fix^{+}) alleles of *NCR-α* or *NCR-β* into the homozygous $NFS1^{-/-}$ background. To our surprise, all of the nodules expressing the transgenes retained Fix^{-} (Fig. S4 *A* and *B*). Consistent with this observation, CRISPR/Cas9-based knockout of the *NCR-α* (Fig. S5 *A* and *C*) or *NCR-β* (Fig. S5 *B* and *D*) alleles in the homozygous $NFS1^{+/+}$ background did not alter the Fix^{+} phenotype. These results indicate that *NCR-α* and *NCR-β* of DZA315 are not essential for forming Fix^{+} nodules by Rm41.

We then used CRISPR/Cas9 to mutate the resident (A17) alleles of *NCR-α* or *NCR-β* in the $NFS1^{-/-}$ background of RHL-NFS1. Intriguingly, the knockout of *NCR-α* converted the Fix^{-} phenotype to Fix^{+} (Fig. 3*B* and Fig. S6*A*) whereas the knockout of *NCR-β* did not change the Fix^{-} phenotype (Fig. 3*C* and Fig. S6*B*). Furthermore, transferring the *NCR-α* allele of A17 into the $NFS1^{+/+}$ genotype resulted in the formation of Fix^{-} nodules on the transgenic roots (Fig. 3*D*). Taken together, our results indicate that the A17 allele of *NCR-α* corresponds to $NFS1^{-}$ and acts dominantly to block nitrogen fixation by *S. meliloti* Rm41.

NFS1 encodes a protein of 68 amino acids (aa), consisting of a predicted 26-aa signal peptide in the N terminus. Cleaving off the signal peptide would produce a 42-aa anionic peptide with six cysteines at the conserved positions (Fig. 4*A*). There are three amino acid substitutions that distinguish between $NFS1^{-}$ (A17) and $NFS1^{+}$ (DZA315) peptides. Sequence analyses of additional *Medicago* accessions, including 22 *M. truncatula* and one *Medicago sativa* (alfalfa) lines, revealed another peptide isoform

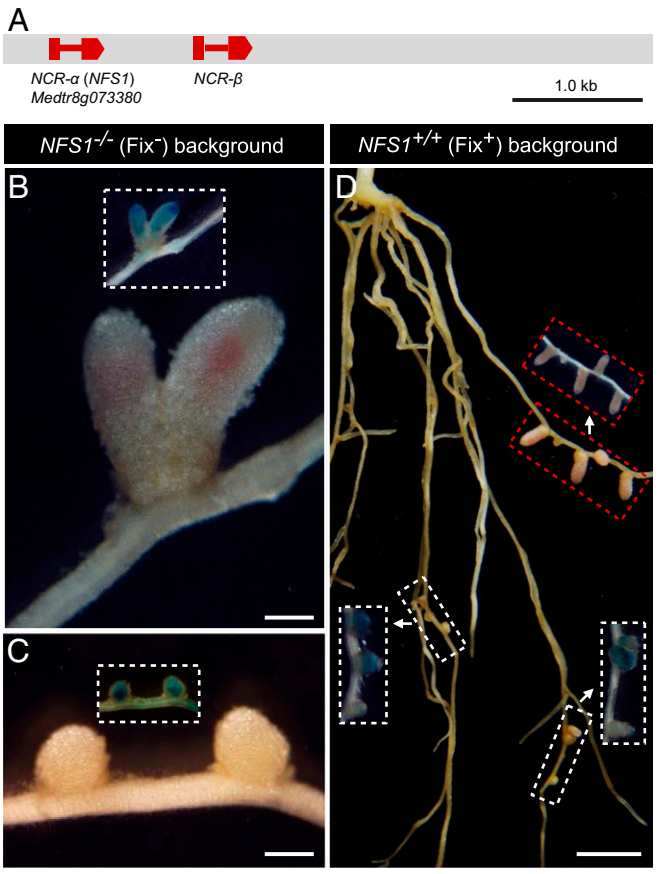

Fig. 3. Functional analysis of the A17 alleles of the candidate genes *NCR-α* and *NCR-β* in the near-isogenic background of RHL-NFS1. (*A*) *NFS1* was mapped to a 4.9-kb genomic region on chromosome 8 containing two predicted genes, *NCR-α* and *NCR-β*. Boxes represent exons, and the lines between them are introns. (*B*) CRISPR/Cas9-mediated knockout of the A17 allele of *NCR-α* in the $NFS1^{-/-}$ (Fix^{-}) background converted the Fix^{-} phenotype to Fix^{+}. (*C*) Knockout of the A17 allele of *NCR-β* in the $NFS1^{-/-}$ (Fix^{-}) background retained the Fix^{-} phenotype. (*D*) Transgenic hairy roots expressing the A17 allele of *NCR-α* in the $NFS1^{+/+}$ (Fix^{+}) background led to the formation of Fix^{-} nodules (indicated by the white boxes) whereas the nontransgenic roots formed Fix^{+} nodules (marked by the red boxes). *Inset* figures show GUS staining of the same nodules/roots in the main panel, as an indicator for the transgenic roots. (Scale bars: *B* and *C*, 500 μm; *D*, 0.5 cm.)

represented by A20 (Fix^{+}) that differs with the DZA315 peptide by one amino acid substitution (Fig. 4*A* and Fig. S7).

A sample of the 25 plant genotypes that capture a wide range of genetic diversity present in natural populations of *M. truncatula* (24) yields an $NFS1^{-}$ allele frequency of 0.08 (2 out of 25), suggesting that this allele is selected against in natural populations. Twelve of the 25 genotypes express the A20 ($NFS1^{+}$) isoform, but, of these 12 genotypes, 3 are Fix^{-} (Fig. S7), consistent with our prediction that the incompatibility with Rm41 is controlled by multiple loci in *M. truncatula*. Interestingly, the negative effect of $NFS1^{-}$ on symbiosis is dependent on the host genetic background. For example, in the RIL population, 13 of the 92 Fix^{+} RILs carry the homozygous $NFS1^{-/-}$ genotype (Table S1), suggesting that the negative role of $NFS1^{-}$ in symbiotic persistence is suppressed in these genetic backgrounds.

In addition to the *NFS1* locus, we identified and cloned a second locus termed *NFS2* (25). *NFS1* and *NFS2* are physically linked on chromosome 8, separated from each other by ~7.7 Mb (Fig. S8). *NFS2* also encodes an NCR peptide and shows the same inheritance pattern as *NFS1*. However, the residual heterozygous line RHL-NFS2 that segregated at the *NFS2* locus

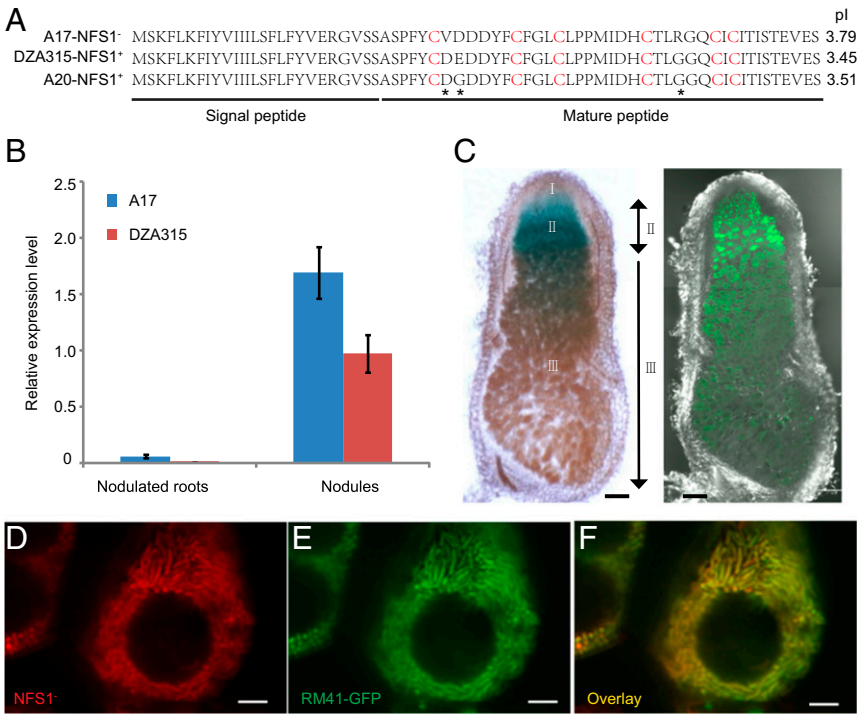

Fig. 4. Sequence, expression, and cellular localization of NFS1. (*A*) Alignment of NFS1 peptide isoforms. The conserved cysteine residues are highlighted in red. Asterisks indicate the amino acid substitution sites. The isoelectric point (pI) of each peptide is indicated. (*B*) *NFS1* is predominantly expressed in root nodules. (*C*) A promoter-GUS assay indicates that *NFS1*$^{-}$ is predominantly expressed in the proximal half of the infection zone (II) and the transition between the infection and fixation zones. The two images were from the same section before (*Right*) and after (*Left*) GUS-staining. I, meristem zone; II, infection zone; III, nitrogen fixation zone. The confocal image (*Right*) was prepared by merging two separate photographs. (Scale bars: 100 μm.) (*D–F*) Localization of NFS1^{-}-mCHERRY (*D*), GFP-tagged bacteroids (*E*), and an overlay (*F*) in a symbiotic cell from the transition zone, showing that the NFS1^{-} peptides colocalized with the symbiosomes before the bacteroids were killed. (Scale bars: 5 μm.)

carries homozygous *NFS1* alleles of A17 (*NFS1*$^{-/-}$), further indicating that the antisymbiotic activity of *NFS1*$^{-}$ is counteracted by other genes in this genetic background. Similar to the *NFS1* locus, the *NFS2*$^{-}$ allele also acts in a context-dependent manner; for example, *NFS2*$^{-}$ is not essential for forming Fix^{-} nodules in the A17 background, even though it is required in the RHL-NFS2 background (25).

When inoculated with Rm41, the expression of the *NFS1*$^{-}$ and *NFS1*$^{+}$ alleles was mostly confined to root nodules and barely detectable in the nodulated roots (Fig. 4*B*). A promoter-GUS (β-glucuronidase) assay indicated that *NFS1*$^{+}$ is predominantly expressed in the cell layers around the boundary of the infection and fixation zones in the Fix^{+} nodules (Fig. 4*C*). A similar expression profile was also revealed by an analysis of the RNA-seq data derived from the Fix^{+} nodules induced by the compatible strains Rm1021 and Rm2011 on A17 roots (26) (Fig. S9), suggesting that the expression pattern of *NFS1* is independent of the bacterial strain inoculated. To determine whether NFS1^{-} colocalizes with bacteroids, we generated a translational fusion construct of *NFS1*$^{-}$-mCherry under the control of its own promoter. Transferring this construct into the *NFS1*$^{+/+}$ (Fix^{+}) background of RHL-NFS1 converted the Fix^{+} phenotype to Fix^{-} and demonstrated that NFS1^{-} localized to the symbiosomes in the cells at the transition between the infection and fixation zone where the bacteria had not yet been killed (Fig. 4 *D–F*). However, the bacteroids were generally unable to survive the presence of the peptides in the fixation zone (Fig. S10).

NCRs are structurally similar to the defensin-like antimicrobial peptides (23). Despite being essential for bacterial differentiation and intracellular survival in nodule cells, several synthetic NCR peptides have been demonstrated to have in vitro bactericidal activities (18–20). Because our attempts to synthesize the NFS1 peptides were unsuccessful, we tested the antimicrobial activity of the peptides by expressing the *NFS1*$^{+}$ (DZA315) or *NFS1*$^{-}$ (A17) allele in Rm41 through an introduced plasmid (pSRKTc) driven by an inducible *lac* promoter (27). Induced expression of *NFS1*$^{-}$ or *NFS1*$^{+}$ in Rm41 significantly reduced the bacterial growth rate, as indicated by the decrease of colony size in plating assays (Fig. 5*A*). Similar antimicrobial activity of the peptides was also observed on *S. medicae* ABS7, a

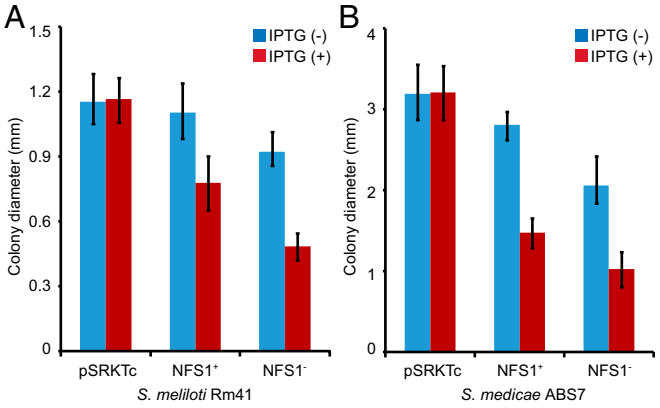

Fig. 5. Assay for antibacterial activity of the NFS1 peptides on *S. meliloti* Rm41 (*A*) and *S. medicae* ABS7 (*B*). The bacteria containing the pSRKTc vector grew at a similar rate, regardless of the presence (+) or absence (–) of isopropyl β-D-1-thiogalactopyranoside (IPTG). However, induced expression of NFS1^{+} or NFS1^{-} by IPTG both significantly ($P < 0.0001$) slowed down the bacterial growth, resulting in smaller colonies.

strain that forms Fix$^+$ nodules on both A17 and DZA315 (Fig. 5*B*). These tests show that the peptides have the antibacterial property but this property does not necessarily reflect their in planta function because of the involvement of other genes in the genetic background.

Rhizobial factors such as NCR-degrading host-range restriction peptidases (HrrPs) play roles in late-stage compatibility (21). We suspected that the symbiotic effects of the *NFS1* alleles might be altered by expressing in Rm41 the HrrP peptidase from *S. meliloti* B800 (21). However, Rm41 transformed with the *HrrP* gene exhibited no changes in symbiotic outcomes with A17 or DZA315. Nevertheless, one can imagine genetic changes in Rm41 (by mutation or gene acquisition) that might expand its compatibility to the NCR peptide ensemble of a currently incompatible host such as A17. It remains to be determined what bacterial components are responsible for differential responses to a specific ensemble of NCR peptides encoded by the host.

Conclusion

Bacterial internalization is associated with host expression of hundreds of diverse NCR peptides in *M. truncatula* (16–20). This highly orchestrated molecular event has been associated with bacterial differentiation into nitrogen-fixing bacteroids although the requirement for such a complex arsenal of peptides has been a matter of speculation. It was hypothesized that NCRs evolved from defensin-like antimicrobial peptides to impose morphological and physiological changes on the endosymbionts so that the bacteria can fix nitrogen more efficiently (3, 18, 28, 29). If this hypothesis is the case, then the legumes did not achieve this evolutionary advantage without sacrifice because certain microsymbionts are apparently unable to survive the bactericidal effects of some NCRs. Thus, this host-dominated strategy must be finely tuned so that the NCR peptides not only keep the bacteria under control but also ensure a prolonged life span for bacteria to fix nitrogen.

The effects of individual NCRs on symbiosis are strain-specific and also dependent on the presence of other interacting factors in the host genome. This genotype-by-genotype interaction likely drives a coevolutionary process that is responsible for the amplification and diversification of NCR-encoding genes. We propose that a concerted action of a large number of polymorphic NCRs with strain-specific control of bacterial differentiation and/or survival explains the existing tremendous natural variation in nitrogen fixation efficiency between different plant–strain combinations. Symbiotic benefits are realized only when appropriate genetic alignment between symbionts is achieved.

Materials and Methods

Plant Materials, Nodulation Assay, and Genetic Mapping. The *M. truncatula* seeds used in this study were provided by Jean-Marie Prosperi, Amélioration Génétique et Adaptation des Plantes Méditerranéennes et Tropicales, Institut National de la Recherche Agronomique, Montpellier, France. Plants were grown in a 50–50 mixture of vermiculite and Turface in a growth chamber programmed for 16 h light at 22 °C and 8 h dark at 20 °C. For the nodulation assay, roots of 1-wk-old seedlings were flood-inoculated with *S. meliloti* Rm41 or *S. medicae* ABS7. Nitrogen-fixing phenotypes were recorded 4 wk postinoculation. Genetic mapping was based on single nucleotide polymorphisms (SNPs) identified between the two parental genotypes Jemalong A17 and DZA315. SNPs were genotyped either by converting to cleaved amplified polymorphic sequences (CAPS) markers or by direct sequencing.

Plasmids and Vectors. For complementation tests, the genomic DNA of the candidate genes was cloned into the pCAMBIA1305.1 vector using the In-Fusion Advantage PCR Cloning Kits (Clontech). The expression of these genes was driven by their native promoters. The vectors contained a GUSPlus gene expression cassette, which facilitated the identification of the transgenic roots. For developing the CRISPR/Cas9 gene knockout constructs, we used the pKSE401 vector described by Xing et al. (30). Two pairs of oligos were designed to specifically target *NCR-α* and *NCR-β*, respectively. For *NCR-α*, we used the oligos 5′ATTGTTGAAAGAGGTGTAAGCTC3′ and 5′AAACGAGCTTACACCTCTTTCAA3′. For *NCR-β*, we used the oligos 5′ATTGTTGTAAGGGATGAAAGCTC3′ and 5′AAACGAGCTTTCATCCCTTACAA3′. The underlined sequences represent the targeted sites. The oligo pairs were first annealed to produce a double-stranded fragment with 4-nt 5′ overhangs at both ends, and then ligated into the BsaI-digested pKSE401 vector. We also amplified the GUSPlus gene cassette from pCAMBIA1305.1 and ligated into the pKSE401 vector using the In-Fusion Advantage PCR Cloning Kits (Clontech).

For the promoter-GUS assay, a 1.6-kb fragment upstream of the translation start site of *NCR-α* was first cloned into the pDONR/Zeo vector (Invitrogen) and then subcloned into the pMDC163 vector using the Gateway cloning system (Invitrogen). The *NCR-α*/mCherry translational fusion construct was developed by in-frame fusion between the second exon of *NCR-α* and the mCherry coding sequence in pCAMBIA1305.1.

Hairy Root Transformation and Analysis of Transgenic Roots. Plasmids were transformed into the *Agrobacterium rhizogenes* strain ARqua1, and hairy root transformations were performed according to the procedures described by Boisson-Dernier et al. (31). The transgenic roots were first identified by GUS staining of a small portion of the root segments. For CRISPR/Cas9-based knockout experiments, transgenic roots were subjected to DNA isolation, PCR amplification, and DNA sequencing to validate the targeted DNA insertions/deletions. If the initial sequencing indicated the presence of multiple heterogeneous mutant alleles, the PCR product was ligated into the pGEM T-Easy Vector System (Promega), and 10 to 15 clones were selected for sequencing.

Analysis of Gene Expression. Total RNA was isolated by the Qiagen Plant RNeasy Mini Kit. Two micrograms of RNA were used to perform RT-PCR reactions using Moloney murine leukemia virus reverse transcriptase (Invitrogen) in a 20-μL reaction mixture. Two microliters of the RT reaction were used as a template in a 20-μL PCR solution. Real-time quantitative PCR was carried out according to the instructions of the SsoAdvanced SYBR Green Supermix Kit (Bio-Rad) using a CFX Connect Real-time System (Bio-Rad). The reaction mixture was heated at 95 °C for 10 min, and then followed by 40 cycles of 95 °C for 15 s, 61 °C for 15 s, and 72 °C for 30 s. Three biological replicates were used in all of the experiments. The PCR primer pair used for *NCR-α* was 5′TATGTTATTATCATTTTGAGTTTCC3′ and 5′GTTATACATATACATTGACCACGAA3′ and, for *Mt-ubiquitin*, was 5′GCAGATAGACACGCTGGGA3′ and 5′CAGTCTTCAAAACTCTTGGGCAG3′.

Microscopy. For the analysis of the structure of the Fix$^+$ and Fix$^-$ nodules, the tissue was fixed in 4% (wt/vol) paraformaldehyde with 3% (wt/vol) glutaraldehyde in 50 mM phosphate buffer (pH7.4), postfixed with 1% (wt/vol) of OsO4, embedded in LR White resin according to the supplier recommendations and polymerized at 60 °C. For light microscopy, semithin sections (0.6 μm) were cut using a Leica Ultracut microtome and counterstained by 0.05% toluidine blue. For electron microscopy, thin sections (60 nm) were cut and contrasted with 2% (wt/vol) aqueous uranyl acetate and lead citrate. Sections were examined using a JEOL JEM 2100 transmission electron microscope equipped with a Gatan US4000 4K×4K camera. For fluorescence microscopy, nodules infected by GFP-tagged Rm41 or expressing an mCHERRY-fused proteins were hand-sectioned using double-edged razor-blades and mounted on microscope slides in 0.1 M phosphate buffer (pH 7.4) containing 25 mg/mL sucrose. Sectioned nodules were examined using an FV1000 confocal laser scanning microscope (Olympus).

Assay for Antimicrobial Activity of the NFS1 Peptides. Antimicrobial activity of the NFS1 peptides was assayed by expressing the *NFS1*$^-$ (A17) or *NFS1*$^+$ (DZA315) allele in *S. meliloti* Rm41 and *S. medicae* ABS7. For this purpose, the coding sequences of the *NFS1* alleles were cloned into the broad–host-range expression vector pSRKTc between the NdeI and KpnI sites (27). The pSRKTc vector contains a *lacI*^{q}-*lac* promoter–operator complex in which the cloned genes are strongly repressed in the absence of inducer. The plasmids were mobilized into the rhizobial strains through either electroporation (for ABS7) or triparental mating (for Rm41) with the helper plasmid pRK600. Cultures of Rm41 or ABS7 (OD_{600} = 0.4), each harboring pSRKTc, pSRKTc-*NFS1*$^-$, or pSRKTc-*NFS1*$^+$, were diluted to 10^{-6}. One hundred microliters of each dilution was plated on to the agarose plates with TY medium and appropriate antibiotics in the presence or absence of 4 mM isopropyl β-D-1-thiogalactopyranoside (IPTG). The colony size was evaluated at 3 d after incubation at 30 °C.

ACKNOWLEDGMENTS. We thank E. Kondorosi, P. Kalo, and A. Kereszt for helpful comments on the manuscript; and J. Prosperi (Institut National de la Recherche Agronomique), L. Gentzbittel (Université de Toulouse), P. Mergaert (Université Paris-Sud), S. Long (Stanford University), and C. Faqua (Indiana University) for providing materials. This work was supported by US Department of Agriculture/National Institute of Food and Agriculture Grants 2014-67013-21573 (to H.Z.) and 2015-67013-22915 (to J.S.G.), Kentucky Science and Engineer Foundation Grant 2615-RDE-015 (to H.Z.), US National Science Foundation Grant IOS-1054980 (to J.S.G.), and European Research Council Advanced Grant ERC-2011-AdG-294790 (to T.B.). Confocal microscopy work was supported by the US National Science Foundation under Cooperative Agreement 1355438.

1. Oldroyd GE, Murray JD, Poole PS, Downie JA (2011) The rules of engagement in the legume-rhizobial symbiosis. *Annu Rev Genet* 45:119–144.
2. Jones KM, Kobayashi H, Davies BW, Taga ME, Walker GC (2007) How rhizobial symbionts invade plants: The *Sinorhizobium-Medicago* model. *Nat Rev Microbiol* 5:619–633.
3. Kereszt A, Mergaert P, Kondorosi E (2011) Bacteroid development in legume nodules: Evolution of mutual benefit or of sacrificial victims? *Mol Plant Microbe Interact* 24: 1300–1309.
4. Perret X, Staehelin C, Broughton WJ (2000) Molecular basis of symbiotic promiscuity. *Microbiol Mol Biol Rev* 64:180–201.
5. Wang D, Yang S, Tang F, Zhu H (2012) Symbiosis specificity in the legume: Rhizobial mutualism. *Cell Microbiol* 14:334–342.
6. Pacios Bras C, et al. (2000) A *Lotus japonicus* nodulation system based on heterologous expression of the fucosyl transferase NodZ and the acetyl transferase NolL in *Rhizobium leguminosarum*. *Mol Plant Microbe Interact* 13:475–479.
7. Radutoiu S, et al. (2007) LysM domains mediate lipochitin-oligosaccharide recognition and Nfr genes extend the symbiotic host range. *EMBO J* 26:3923–3935.
8. Kawaharada Y, et al. (2015) Receptor-mediated exopolysaccharide perception controls bacterial infection. *Nature* 523:308–312.
9. Deakin WJ, Broughton WJ (2009) Symbiotic use of pathogenic strategies: Rhizobial protein secretion systems. *Nat Rev Microbiol* 7:312–320.
10. Yang S, Tang F, Gao M, Krishnan HB, Zhu H (2010) *R* gene-controlled host specificity in the legume-rhizobia symbiosis. *Proc Natl Acad Sci USA* 107:18735–18740.
11. Tang F, Yang S, Liu J, Zhu H (2016) *Rj4*, a gene controlling nodulation specificity in soybeans, encodes a thaumatin-like protein but not the one previously reported. *Plant Physiol* 170:26–32.
12. Tirichine L, de Billy F, Huguet T (2000) *Mtsym6*, a gene conditioning Sinorhizobium strain-specific nitrogen fixation in *Medicago truncatula*. *Plant Physiol* 123:845–851.
13. Liu J, Yang S, Zheng Q, Zhu H (2014) Identification of a dominant gene in *Medicago truncatula* that restricts nodulation by *Sinorhizobium meliloti* strain Rm41. *BMC Plant Biol* 14:167.
14. Mergaert P, et al. (2006) Eukaryotic control on bacterial cell cycle and differentiation in the *Rhizobium*-legume symbiosis. *Proc Natl Acad Sci USA* 103:5230–5235.
15. Julier B, et al. (2007) Identification of quantitative trait loci influencing aerial morphogenesis in the model legume *Medicago truncatula*. *Theor Appl Genet* 114: 1391–1406.
16. Mergaert P, et al. (2003) A novel family in *Medicago truncatula* consisting of more than 300 nodule-specific genes coding for small, secreted polypeptides with conserved cysteine motifs. *Plant Physiol* 132:161–173.
17. Wang D, et al. (2010) A nodule-specific protein secretory pathway required for nitrogen-fixing symbiosis. *Science* 327:1126–1129.
18. Van de Velde W, et al. (2010) Plant peptides govern terminal differentiation of bacteria in symbiosis. *Science* 327:1122–1126.
19. Kim M, et al. (2015) An antimicrobial peptide essential for bacterial survival in the nitrogen-fixing symbiosis. *Proc Natl Acad Sci USA* 112:15238–15243.
20. Horváth B, et al. (2015) Loss of the nodule-specific cysteine rich peptide, NCR169, abolishes symbiotic nitrogen fixation in the *Medicago truncatula dnf7* mutant. *Proc Natl Acad Sci USA* 112:15232–15237.
21. Price PA, et al. (2015) Rhizobial peptidase HrrP cleaves host-encoded signaling peptides and mediates symbiotic compatibility. *Proc Natl Acad Sci USA* 112:15244–15249.
22. Farkas A, et al. (2014) *Medicago truncatula* symbiotic peptide NCR247 contributes to bacteroid differentiation through multiple mechanisms. *Proc Natl Acad Sci USA* 111: 5183–5188.
23. Maróti G, Downie JA, Kondorosi É (2015) Plant cysteine-rich peptides that inhibit pathogen growth and control rhizobial differentiation in legume nodules. *Curr Opin Plant Biol* 26:57–63.
24. Stanton-Geddes J, et al. (2013) Candidate genes and genetic architecture of symbiotic and agronomic traits revealed by whole-genome, sequence-based association genetics in *Medicago truncatula*. *PLoS One* 8:e65688.
25. Wang Q, et al. (2017) Host-secreted antimicrobial peptide enforces symbiotic selectivity in *Medicago truncatula*. *Proc Natl Acad Sci USA* 114:6854–6859.
26. Roux B, et al. (2014) An integrated analysis of plant and bacterial gene expression in symbiotic root nodules using laser-capture microdissection coupled to RNA sequencing. *Plant J* 77:817–837.
27. Khan SR, Gaines J, Roop RM, 2nd, Farrand SK (2008) Broad-host-range expression vectors with tightly regulated promoters and their use to examine the influence of TraR and TraM expression on Ti plasmid quorum sensing. *Appl Environ Microbiol* 74: 5053–5062.
28. Oono R, Denison RF (2010) Comparing symbiotic efficiency between swollen versus nonswollen rhizobial bacteroids. *Plant Physiol* 154:1541–1548.
29. Oono R, Schmitt I, Sprent JI, Denison RF (2010) Multiple evolutionary origins of legume traits leading to extreme rhizobial differentiation. *New Phytol* 187:508–520.
30. Xing HL, et al. (2014) A CRISPR/Cas9 toolkit for multiplex genome editing in plants. *BMC Plant Biol* 14:327.
31. Boisson-Dernier A, et al. (2001) *Agrobacterium rhizogenes*-transformed roots of *Medicago truncatula* for the study of nitrogen-fixing and endomycorrhizal symbiotic associations. *Mol Plant Microbe Interact* 14:695–700.
32. Tang H, et al. (2014) An improved genome release (version Mt4.0) for the model legume *Medicago truncatula*. *BMC Genomics* 15:312.